

Research Article

Experimental Study of Vibrations of Gerbil Tympanic Membrane with Closed Middle Ear Cavity

NIMA MAFTOON¹, W. ROBERT J. FUNNELL^{1,3}, SAM J. DANIEL^{2,3}, AND WILLEM F. DECRAEMER⁴,

¹*Department of BioMedical Engineering, McGill University, Montréal, Canada*

²*Department of Pediatric Surgery, McGill University, Montréal, Canada*

³*Department of Otolaryngology—Head and Neck Surgery, McGill University, Montréal, Canada*

⁴*Biomedical Physics, University of Antwerp, Antwerp, Belgium*

Received: 2 November 2012; Accepted: 31 March 2013; Online publication: 27 April 2013

ABSTRACT

The purpose of the present work is to investigate the spatial vibration pattern of the gerbil tympanic membrane (TM) as a function of frequency. In vivo vibration measurements were done at several locations on the pars flaccida and pars tensa, and along the manubrium, on surgically exposed gerbil TMs with closed middle ear cavities. A laser Doppler vibrometer was used to measure motions in response to audio frequency sine sweeps in the ear canal. Data are presented for two different pars flaccida conditions: naturally flat and retracted into the middle ear cavity. Resonance of the flat pars flaccida causes a minimum and a shallow maximum in the displacement magnitude of the manubrium and pars tensa at low frequencies. Compared with a flat pars flaccida, a retracted pars flaccida has much lower displacement magnitudes at low frequencies and does not affect the responses of the other points. All manubrial and pars tensa points show a broad resonance in the range of 1.6 to 2 kHz. Above this resonance, the displacement magnitudes of manubrial points, including the umbo, roll off with substantial irregularities. The manubrial points show an increasing displacement magnitude from the lateral process toward the umbo. Above 5 kHz, phase differences between points along the manubrium start to become more evident, which may indicate flexing of the tip of the manubrium or a change in the vibration mode of the malleus. At low

frequencies, points on the posterior side of the pars tensa tend to show larger displacements than those on the anterior side. The simple low-frequency vibration pattern of the pars tensa becomes more complex at higher frequencies, with the breakup occurring at between 1.8 and 2.8 kHz. These observations will be important for the development and validation of middle ear finite-element models for the gerbil.

Keywords: middle ear, pars tensa, pars flaccida, manubrium, vibration pattern, laser Doppler vibrometry

INTRODUCTION

Understanding the response of the middle ear to sound stimuli is highly dependent on knowledge of the tympanic membrane (TM) vibrations and they have been the subject of a number of studies, with laser-based methods being particularly valuable. Tonndorf and Khanna (1972) and Khanna and Tonndorf (1972) were the first to study vibration patterns of the human and cat TM by time-averaged laser holography, at frequencies up to 5 and 6 kHz, respectively. They observed that, in both species, the maximum displacement happens in the posterior region, and for frequencies beyond 2.5 kHz, the simple low-frequency vibration pattern starts to break up and vibration patterns become more complex. Funnell and Laszlo (1982) reviewed other applications of holography (as well as other techniques). Later, Ishihara (1989) observed that the breakup frequency

Correspondence to: W. Robert J. Funnell • Department of BioMedical Engineering • McGill University • 3775 rue University, Montreal, QC H3A 2B4, Canada Telephone: +1-514-398-6739; fax: +1-514-398-7461; e-mail: robert.funnell@mcgill.ca

of the human TM “was not affected much” by the cross-sectional area of the aditus ad antrum, the sound pressure level, or the volume of the middle ear cavity. Okano (1990), Suehiro (1990), and Maeta (1991) reported breakup frequencies of 3 kHz for the posterior part and 4 kHz for the anterior part of the dog TM. Wada et al. (2002) used time-averaged laser speckle interferometry to study guinea pig TM vibrations up to 4 kHz. It was seen that complex vibration patterns appear at frequencies above 2.5 kHz.

Point-by-point laser interferometry provides more precise magnitude and phase information than do holographic techniques. Konrádsson et al. (1987) studied vibration of the human TM using scanning laser Doppler vibrometry (LDV) and presented data at 578, 3,107, and 3,113 Hz that were consistent with earlier studies. Decraemer et al. (1989) utilized a homodyne laser interferometer and reported the phase and magnitude for a wide frequency range (130 Hz to 20 kHz) for a few points on the cat pars tensa and manubrium. They observed that, up to 1 kHz, all points on the pars tensa move almost in phase, but beyond that frequency, the phase differences increase and, for frequencies above 5 kHz, each point moves very differently. Decraemer et al. (1999) used an improved interferometer so that the measurements could be done without the need for reflective objects to increase the signal-to-noise ratio, allowing them to measure TM vibrations with a high spatial resolution. They concluded that the motion “looks more like a traveling wave than like a standing wave.”

Recently, Rosowski et al. (2009) used time-averaged holography to study TM vibrations up to 25 kHz in human, cat, and chinchilla. They found increasingly complicated vibration patterns for frequencies higher than 0.8 kHz for chinchilla and 2 kHz for cat and human; for frequencies higher than 1 kHz for chinchilla and 4 kHz for cat and human, the patterns were ring-like. Later, using stroboscopic holography, they were also able to study the phase at a few frequencies in human temporal bones (Cheng et al. 2010) and interpreted their results as indicating a combination of standing waves and “some smaller traveling-wave like components.”

The gerbil is a commonly used species in hearing research. For example, Cohen et al. (1993) investigated the effects of developmental changes on the gerbil umbo velocity response using LDV. Admittance measurements (e.g., Ravicz et al. 1992, 1996; Ravicz and Rosowski 1997; Teoh et al. 1997) and LDV umbo and pars flaccida measurements (e.g., Rosowski et al. 1997, 1999; Lee and Rosowski 2001; Rosowski and Lee 2002) were used to study the gerbil middle and external ears. Quasi-static deformation of the gerbil TM under static pressure was measured in several studies using moiré interferometry (e.g., von Unge et al. 1993;

Dirckx and Decraemer 2001). The gerbil has also been used as an animal model for middle ear infection in several studies (e.g., Fulghum and Marrow 1996; von Unge et al. 1997; Larsson et al. 2005).

Although there have been many experimental studies of the gerbil middle ear, the only measurements of the vibration patterns of the gerbil TM have been those made at a few points on the pars tensa near the umbo by de La Rochefoucauld and Olson (2010) and postmortem studies in our laboratory (Ellaham et al. 2007; Nambiar 2010). The present work, therefore, was performed to investigate the vibrations of the gerbil TM more extensively. Measurements were done in vivo using LDV at several locations on the pars tensa, along the manubrium, and on the pars flaccida. All measurements were done with the middle ear cavity both closed and open, but only closed-cavity data are reported here. The open-cavity observations will be reported in a subsequent paper.

MATERIALS AND METHODS

Preparation

TM vibration was measured in vivo in 12 ears of 11 female Mongolian gerbils (*Meriones unguiculatus*) supplied by Charles River Laboratories (Saint-Constant, Québec, Canada). Body weights were from 64 to 100 g. The study protocol was approved by the McGill University Animal Care Committee.

The animal was weighed and analgesics (buprenorphine 0.05 mg/kg and carprofen 5 mg/kg) were administered subcutaneously. After 15 min, 10 mg/kg xylazine plus 35 mg/kg sodium pentobarbital were given to the animal by intraperitoneal injection. In order to maintain normal body temperature, the gerbil rested on a SnuggleSafe microwave-heated heating pad (Lenric C21 Ltd.) during the whole procedure. A low flow of oxygen was provided to the animal through a tube near the nose. Anesthesia was maintained for several hours of measurements by administering a 5- to 10-mg/kg sodium pentobarbital bolus injection every 45 min. A diluted local anesthetic (lidocaine) was applied on the exposed tissues to control pain locally and to keep the tissue hydrated. A reflex check was done every 5–10 min during the experiment to verify the depth of the anesthesia and, if the animal showed any reaction, an additional dose of 5–10 mg/kg of sodium pentobarbital was injected.

Once the animal reached an appropriate level of anesthesia, the surgery was started. The skin over the skull was excised and a wooden block (2.5×1×1 cm) was attached to the skull with dental cement (IRM, Dentsply Caulk). During measurements, the wooden block was fixed in a positioning device located under

the microscope, which was equipped with a vibrometer sensor head. The soft tissues covering the bulla were removed under an operating microscope. Then, a surgical ear drill was used to remove the bony ear canal and expose the TM. To equalize pressure in the bulla, a ventilation hole was made on the bulla away from the TM; to cancel the acoustic effects of the hole, a 15-cm-long polyethylene tube with an inner diameter of 0.58 mm and an outer diameter of 0.96 mm was inserted into the hole. The ventilation tube was checked for patency at the time of insertion by passing a wire through it. Glass-coated plastic beads of 90 to 150 μm diameter with a density of 1.02 g/cm^3 (Sigma-Aldrich, model G4519) were used as targets for the laser. They increased reflection of the laser beam and thus improved the signal-to-noise ratio of the vibrometer signal. The beads also served as markers of the measurement locations. Placing of the beads was done manually under an operating microscope using a paint brush reduced to a single bristle and there were inevitably some differences in bead positioning from ear to ear. In using beads in our measurements and drawing conclusions from our data, we have assumed that the beads stick perfectly to the TM or manubrium and do not move with respect to the surface. Decraemer et al. (1989) showed that their beads followed the underlying structure, and beads have been used by many groups since then (e.g., Bigelow et al. 1996; Qin et al. 2010).

We used an aluminum acoustic coupler, the interior air space of which had a resonance frequency beyond 10 kHz. A metal washer (9.6 mm O.D., 3.8 mm I.D., 1.1 mm thickness) was attached to the bony ear canal with dental cement and the coupler was attached to the washer, again with dental cement (see Fig. 1). At the other end of the coupler, there was a seat for placing an antireflective coated glass window. Euthanasia with sodium pentobarbital overdose was performed immediately after completion of the data collection.

In a few ears, whose results were excluded from this report, upon exposing the TM, we observed liquid drops on the lateral surface of the TM, sitting on the annulus anteriorly and posteriorly, touching the ear canal wall and extending about 20 % of the distance to the manubrium. These drops, which were associated with significant ripples in the frequency responses, might be caused by exudation due to mechanical stimulation of the ear canal, as observed by Emgård and Hellström (1997) in rats.

Instrumentation

A 128-ms linear sinusoidal sweep from 0.2 to 12.5 kHz was used as the stimulus. Sound was delivered by an ER-2 tubeophone (Etymotic Research) into the acous-

tic coupler through a hole in its wall, and the sound pressure about 2–3 mm away from the TM was picked up by an ER-7C (Etymotic Research) probe microphone connected through another hole in the coupler wall. A third hole was made in the coupler wall for insertion of a ventilation tube to prevent the buildup of pressure and moisture. Both ER-2 and ER-7C have almost flat magnitude responses in the frequency range of interest. The ER-7C probe microphone was calibrated against a Brüel and Kjær 1/4-in. model 4939 condenser microphone using a Brüel and Kjær sound intensity calibrator model 3541. A cubic polynomial and a straight line were fitted to the calibration measurement points below 600 Hz and above 600 Hz, respectively ($R^2=0.995$ for each part).

A single-point LDV (HLV-1000, Polytec) attached to an operating microscope (OPMI 1-H, Zeiss) was used inside a double-walled audiometric examination room (model C-24, Génie Audio, Saint-Laurent, Québec, Canada), which attenuated acoustical noise. Measurements were performed from a single viewing direction. Owing to animal-to-animal variability of the anatomy and of the experimental procedures, there were slight differences between the measurement angles in different ears. The data-acquisition board of the LDV system used delta-sigma-modulating analog-to-digital convertors (e.g., Aziz et al. 2002) with 128 times oversampling, which avoided aliasing. An effective sampling frequency of 25 kHz was used. An extremely flat, linear-phase, low-pass digital filter automatically adjusts its cutoff frequency to remove frequency components above half the requested sampling rate. The frequency range of interest in this study is 200 Hz to 10 kHz.

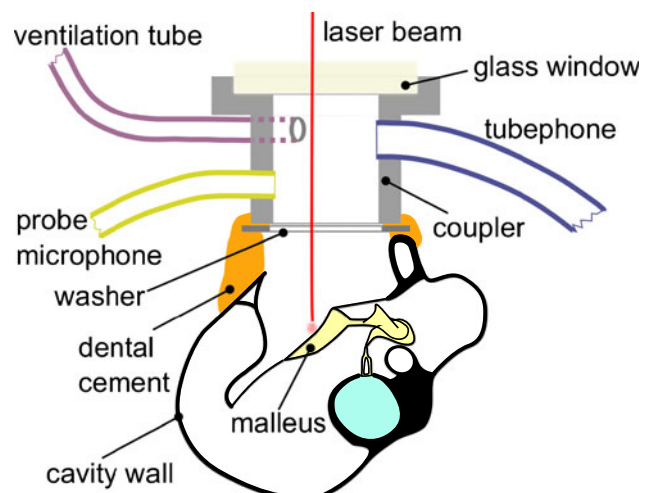


FIG. 1. Schematic diagram showing the acoustic coupler attached to the bony ear canal.

Measurement and analysis procedures

Measurements always started with the middle ear cavity closed, that is, with a small ventilation hole and a ventilation tube in place, as described in the “**Preparation**” section. Before collection of the vibration data began, the probe microphone signal recorded near the TM was inspected to ensure the absence of any acoustical artifacts. To assess the noise floor, the laser beam was pointed at the acoustic coupler or at the cavity wall and the resulting vibration signal was compared with the signal measured from the bead at the umbo. The umbo response was always 30 and 40 dB above the noise floor for frequencies higher than 400 and 600 Hz, respectively. Averaging (20 to 60 times) was used to reduce the low-frequency noise that mainly influenced responses in the frequency range of 200 to 300 Hz. The frequency response function was estimated as the cross-spectral density of the excitation and response signals divided by the power spectral density of the excitation signal. The linearity was checked by varying the sound stimulus amplitude and ensuring that the normalized displacement magnitudes at the umbo remained the same.

To minimize drying effects, we covered the exposed bulla between the soft tissue and the acoustic coupler with a cotton pad moistened with diluted lidocaine solution (our local anesthetic as described in the “**Preparation**” section). The cotton was remoistened every half hour.

In each ear, three or four target beads were placed on the manubrium. One bead was placed approximately at the center of the pars flaccida. Up to three beads were placed on each of the posterior and anterior parts of the pars tensa at the level of the middle of the manubrium, and a few more were placed in the region just posterior, anterior, and inferior to the umbo. The picture of the TM shown on the left-hand side of Figure 2 is focused on the beads inferior to the umbo on the pars tensa, while the picture on the right is focused on the beads at the level of the middle of the manubrium on the pars tensa.

One or two reference beads were always measured at both the start and the end of the measurements on the beads in each region. These reference measurements were used to screen the results both for gradual temporal effects and for possible abrupt changes due to unwanted changes in the system. For points around the umbo on the pars tensa and for points along the manubrium and on the pars flaccida, the umbo was taken as the reference. For points across the manubrium, both the umbo and the closest bead on the manubrium were taken as reference points. The signal from each bead was recorded several times in

a row to confirm repeatability, but only the first recorded signals have been reported here.

A 1,600-line FFT was used to transfer the recorded vibrometer and microphone time domain signals to the frequency domain. A two-pass (forward and reverse) moving-average filter with a window length of five was applied to the real and imaginary parts of the complex signal, and the magnitude and phase responses were then calculated from the filtered complex signal. Such calculated phases are “wrapped” within a range of 360° and their unwrapping can be uncertain in the presence of noise and rapid phase changes. We have checked the configuration and continuity of the Nyquist plots (Cartesian plots of the real part vs. the imaginary part of the complex response) to increase our confidence in the validity of the phase unwrapping process. Examples of Nyquist plots are given in Figure 8 and discussed in the “**Appendix**”.

RESULTS

Effects of using beads

The mass of the beads used as reflective targets may affect the behavior of the TM. The effect of adding beads was assessed in four ears. First, we placed one bead on the umbo and another one on the posterior or anterior part of the pars tensa and recorded the vibrometer signals at these two points; we then successively added up to four more beads near the first bead on the pars tensa. To have access to the pars tensa for adding each bead, we had to remove the acoustic coupler, place the bead, and then seal the coupler again. After the addition of each bead, we measured the motion of the first pars tensa bead and of the umbo bead. These measurements were done postmortem. We observed that, with the addition one at a time of up to four additional beads at one location, structures in the response shifted to higher frequencies due to temporal effects, but differences between the shifted structures remained within 3 dB and 10° . In our regular experiments, we placed no more than three beads on the pars tensa on each side of the manubrium and left some distance between them (about 100 μm) so the response of the pars tensa is not expected to be greatly modified. We were not able to do measurements without any beads on the pars tensa, so these data do not address what happens as the first bead is added to the pars tensa.

In using beads in our measurements and drawing conclusions from our data, we have assumed that the beads stick perfectly to the TM or manubrium and do not move with respect to the surface. Decraemer et al. (1989) showed that the beads follow the underlying

structure, and beads have been used by many groups since then (e.g., Bigelow et al. 1996; Qin et al. 2010).

Repeatability and temporal effects

Our data show a high degree of short-term repeatability in all ears. Except on very rare occasions, the repeat average magnitudes and phases within 5 min were within 1 dB and 3° of the first average, except above the breakup frequency on the pars tensa where they were usually within 2 dB and 7°. For the sharpest features, the differences were sometimes up to 5 dB and 12°, but the shapes of the frequency responses were essentially unchanged.

Dehydration of the middle ear structures is probably one of the main mechanisms that affect long-term repeatability. Drying is caused by altering the normal physiological conditions, by removal of the cartilaginous ear canal and the soft tissues covering the bulla, and manifests itself in the frequency response data as a decrease in magnitude and a frequency shift of the response features to higher frequencies (Voss et al. 2000; Ellaham et al. 2007). In the closed-cavity condition, over a time span of 90 min, most features of the umbo response typically showed a maximum shift of about 2 Hz/min to higher frequencies, a maximum magnitude decrease of about 0.2 %/min, and a maximum phase change of about 0.02°/min over the entire frequency range of interest. The umbo response feature caused by the pars flaccida, consisting of a magnitude minimum and a phase maximum as discussed in the “Low frequencies” section under “Umbo and pars flaccida vibrations”, moved to higher frequencies at a somewhat higher rate (approximately 3 Hz/min). Teoh et al. (1997) also reported faster changes with drying for this feature.

Umbo and pars flaccida vibrations

The response of the umbo is better understood when it is compared with the pars flaccida response, so we present both responses together. Responses are reported for two different pars flaccida conditions: when it is naturally flat and when it is retracted into the middle ear cavity.

Low frequencies. In some of our experiments, the normally flat pars flaccida was retracted into the middle ear cavity. A retracted pars flaccida has an obvious inverted dome-like geometry when examined under the microscope. Typical responses of a flat pars flaccida (gerbil K) and of a retracted pars flaccida (gerbil J) are presented in Figure 3, together with the corresponding umbo responses. In both the flat case and the retracted case, the pars flaccida and the umbo both had a flat magnitude response below 300 Hz and both had a phase of about 0° at up to 700 Hz. The response of the flat pars flaccida in Figure 3 shows a resonance peak at 850 Hz with a width (full width at half maximum) of 220 Hz. In the ears with a flat pars flaccida, the resonance peak was observed to be between 500 and 900 Hz with a width of 140 to 270 Hz. The resonance of a flat pars flaccida corresponds to a minimum and a more or less shallow maximum in the umbo magnitude response, seen at 750 and 950 Hz, respectively, in Figure 3, and a maximum in the umbo phase response, seen at 840 Hz in Figure 3. In contrast, the response of the retracted pars flaccida in Figure 3 shows a gentle increase in magnitude from 300 Hz up to a small peak at about 850 Hz. This small peak is located between 850 and 1,700 Hz in different ears with a retracted pars flaccida. In this ear, the almost flat magnitude response of the umbo continues up to about 600 Hz and is then followed by a gentle rise up to about

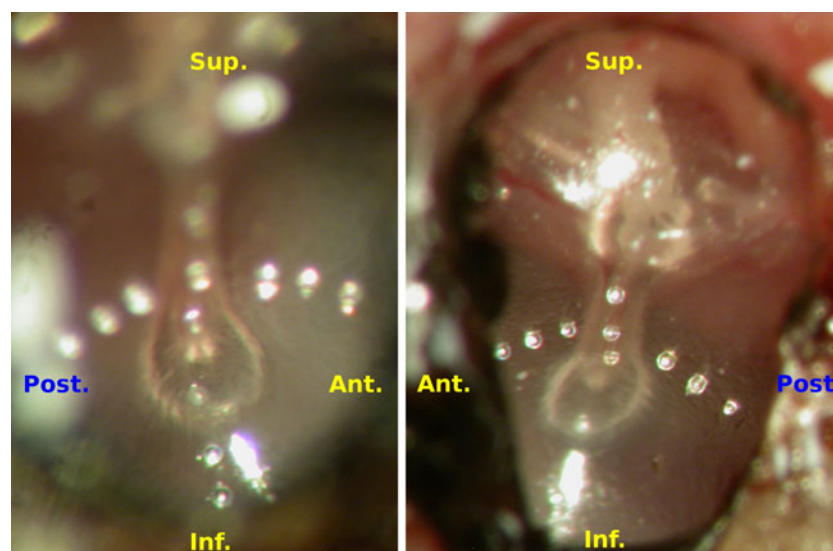


FIG. 2. Lateral views of two TMs. Beads are positioned on the manubrium and the pars tensa.

1,650 Hz. In ears with a retracted pars flaccida like gerbil J in Figure 3, the magnitude response is smaller than that in ears with a flat pars flaccida; it is even smaller than that of the umbo. For example, in Figure 3, at 300 Hz, the displacement magnitude of the retracted pars flaccida is 35 nm/Pa, which is much less than the 500 nm/Pa of the flat pars flaccida and less than the 70 nm/Pa of the umbo.

Figure 4 shows umbo displacement responses for 12 gerbil ears. The responses at low frequencies show an almost flat response, except in a few ears at the lowest frequency, and a phase close to zero (within 30°), which is characteristic of a stiffness-dominated system. In seven ears (gerbils A, B, F, G, I, and J, with dashed lines in Fig. 4), the pars flaccida was retracted into the middle ear cavity. At 300 Hz, the magnitudes in this group ranged between 50 and 90 nm/Pa. In the other five ears (gerbils C, D, E, H, and K, with solid lines in Fig. 4), the pars flaccida was flat and a distinct feature was observed in the umbo magnitude response, with a magnitude minimum between 400 and 700 Hz and a phase maximum between 450 and 750 Hz. The magnitudes at 300 Hz in this group ranged between 45 and 60 nm/Pa, mostly lower than in the group with a retracted pars flaccida. Note that, for gerbil K, the umbo response shown in Figure 4 was measured about 95 min later than the one shown in Figure 3. Temporal effects changed the resonance frequency of the pars flaccida, so in Figure 4, the umbo response feature related to the pars flaccida is about 300 Hz higher in frequency than it is in Figure 3.

The magnitude-minimum/phase-maximum feature in the umbo response became gradually less distinct with a greater degree of retraction. For example, the pars flaccida in gerbil D was partially retracted and a shallow minimum in the umbo magnitude response is still visible at 610 Hz in

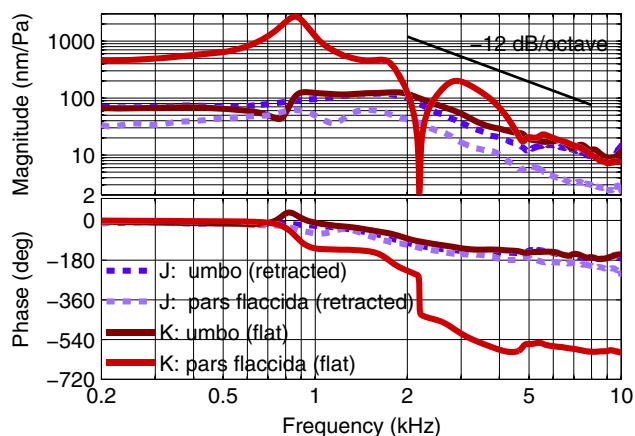


FIG. 3. Displacement response of the center of the pars flaccida and of the umbo, normalized by sound pressure, in two ears. The pars flaccida was retracted in gerbil J (dashed lines) and was flat in gerbil K (solid lines).

Figure 4. During measurements in two ears (C and H), each with an initially flat pars flaccida, we noticed that, over a time interval of about 1 min, the low-frequency umbo magnitude gradually increased and the minimum associated with the pars flaccida resonance disappeared. The effect in gerbil H can be appreciated by comparing Figures 4 and 5.

The low-frequency results provided in Figures 3 and 4 are in general agreement with the findings of Rosowski et al. (1997), Lee and Rosowski (2001), and Rosowski and Lee (2002). In all three studies, the results were reported in terms of velocities, and for comparison with our data, we have converted them to displacements. Except for the results from Rosowski et al. (1997), which are only for one ear, the data from the other studies involved pressure sweeps and can be compared with our results only with caution because the directions of the pressure sweeps affected the observations at zero static pressure. The low-frequency umbo displacement magnitude was reported to be approximately 55 nm/Pa at 200 Hz (Rosowski et al. 1997; Fig. 6), 56.7 ± 6.7 (SEM) nm/Pa at 250 Hz (Lee and Rosowski 2001; Fig. 7, zero static pressure, average of the two pressure sweep directions), and 35 to 48 nm/Pa (95 % confidence interval) at 200 Hz (Rosowski and Lee 2002; Fig. 2, zero static pressure, positive-to-negative sweep). These values are consistent with the range of 45 to 60 nm/Pa that we report here for the umbo displacement magnitude with a flat pars flaccida at 300 Hz. In Rosowski and Lee (2002; Fig. 3, zero static pressure, positive-to-negative sweep), the umbo displacement magnitude with an immobilized pars flaccida was reported to be from about 45 to 60 nm/Pa (95 % confidence interval) at 200 Hz, similar to the range of 50 to 90 nm/Pa that we report here for the umbo response with a retracted pars flaccida at 300 Hz.

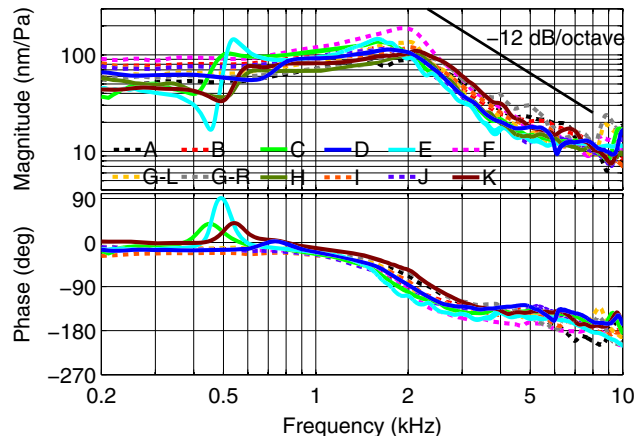


FIG. 4. Umbo displacement response normalized by sound pressure in 12 ears. The responses measured in ears with a flat pars flaccida are shown with solid lines and the responses measured in ears with a retracted pars flaccida are shown with dashed lines.

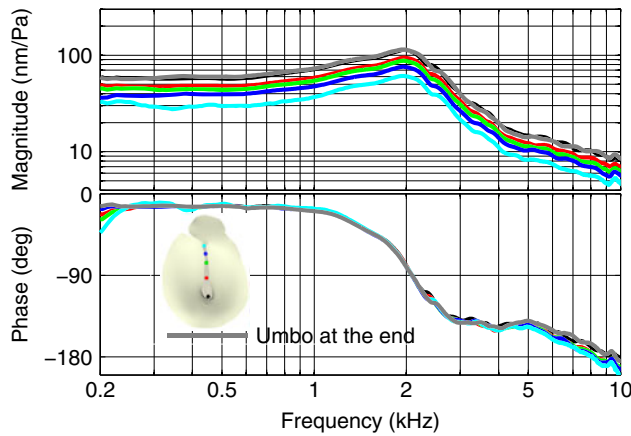


FIG. 5. Displacement response normalized by sound pressure along the manubrium in gerbil H.

Mid and high frequencies. As shown in Figure 3, near and above the resonance of the flat pars flaccida, its phase departs from that of the umbo. The pars flaccida displacement remains higher than that of the umbo up to about 4.5 kHz, except around 2.2 kHz where it shows a sharp and deep antiresonance. This antiresonance was absent in some ears (e.g., gerbil E, not shown here). When the antiresonance is present, it causes a phase shift of almost half a cycle (180°). At higher frequencies, in this animal, the pars flaccida magnitude went down to about the level of that of the umbo, while in other animals, the pars flaccida magnitude was as much as 7.5 dB lower than that of the umbo.

In the response of the retracted pars flaccida of Figure 3, the phase follows the umbo phase closely up to 3.5 kHz, except for a divergence with a minimum at about 1 kHz, but at higher frequencies, the phase difference increases up to about 70° at 10 kHz. The 1-kHz minimum of the divergence in the pars flaccida phase is accompanied by a minimum in the magnitude at a slightly higher frequency. A similar behavior in both magnitude and phase was seen in all ears, with phase minima in the range of 1 to 1.7 kHz.

Figure 4 shows that, for both flat and retracted pars flaccida, the umbo response has a rather broad resonance with a peak between 1.6 and 2.0 kHz. The maximum displacement at the resonance is from 90 to 190 nm/Pa. The ratio of the displacement at the resonance peak to the displacement at the low-frequency asymptote is from 1.6 to 2.1 in different ears. We quantify the width of the resonance as the full width at half maximum of the velocity response. (We use velocity because, for the displacements, the low-frequency magnitude is sometimes greater than the half-maximum magnitude.) The width computed in this way varies from 1.5 to 2.8 kHz in the different ears.

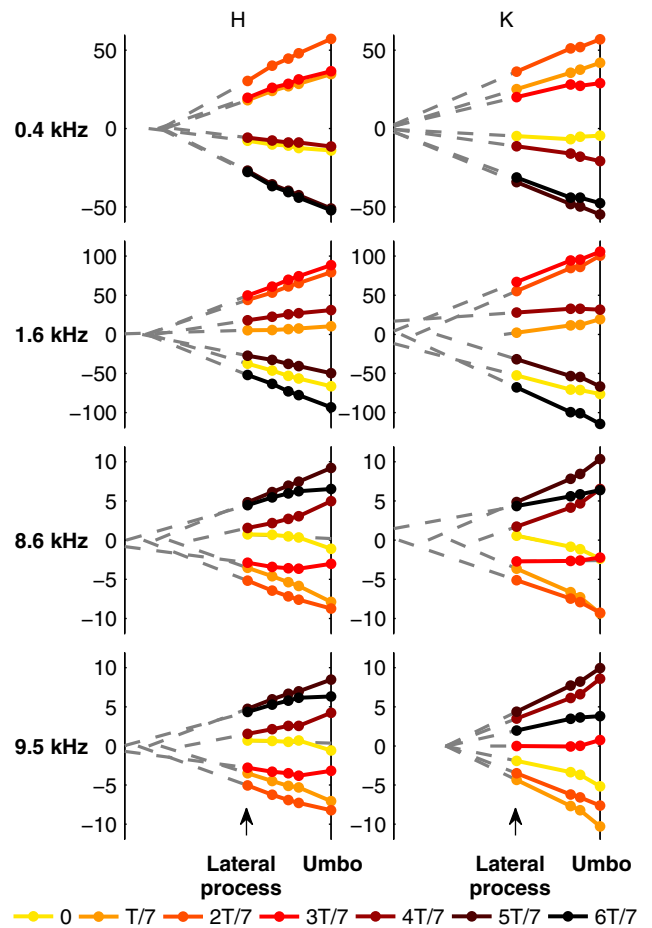


FIG. 6. Sinusoidal motion of the manubrium at seven time instants (multiples of T/7) throughout the cycle in gerbils H and K at frequencies of 400, 1,600, 8,600, and 9,500 Hz.

For frequencies above the resonance frequency, the umbo magnitude generally decreases with increasing frequency, but with substantial irregularities. These irregularities typically have bandwidths of a few hundred hertz, magnitude changes of a few

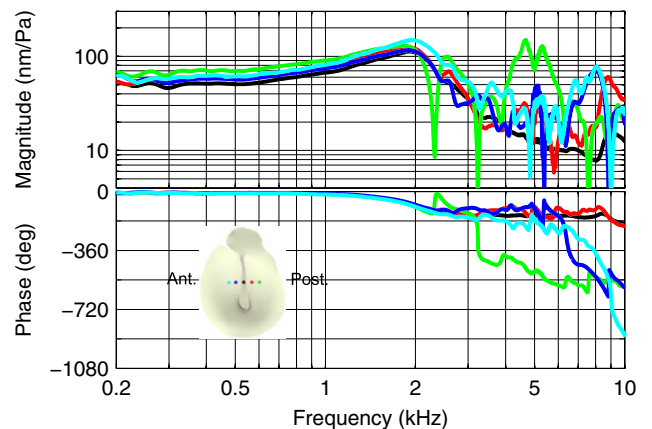


FIG. 7. Pars tensa displacement responses, normalized by sound pressure, at locations in a line perpendicular to the manubrium in the left ear of gerbil G.

decibels, and phase changes of a few tens of degrees; these changes are quite stable in time and are much larger than the short-term variations described in the “Repeatability and temporal effects” section. In the range of 8.5 to 9.1 kHz, three ears (gerbils F and G) show a distinct maximum and six ears (gerbils A, C, D, H, J, and K) show a distinct minimum.

Ravicz et al. (1992) and Teoh et al. (1997) also reported a gerbil middle ear resonance frequency of about 2 kHz in their impedance and admittance measurements. The three studies mentioned in the “Low frequencies” section presented mid-frequency and high-frequency response shapes that, when converted to displacement, are similar to those presented here. At the resonance peak, Rosowski et al. (1997; Fig. 6) reported umbo displacement magnitudes of approximately 110 nm/Pa at about 2.1 kHz, which is consistent with our observed range of 90 to 190 nm/Pa. Other reported values in the literature are 67.0 ± 7.8 (SEM) nm/Pa at 2 kHz (Lee and Rosowski 2001; Fig. 7, zero static pressure, average of the two pressure sweep directions) and 55 to 80 nm/Pa (95 % confidence interval) with normal pars flaccida and 45 to 65 nm/Pa (95 % confidence interval) with immobilized pars flaccida, both between about 1.7 and 2.1 kHz (Rosowski and Lee 2002; zero static pressure, positive-to-negative sweep: Fig. 2, normal pars flaccida; Fig. 3, immobilized pars flaccida). These are lower than the ranges reported in the current study but, as mentioned in the “Low frequencies” section, values from these two studies that involved pressure sweeps can be compared with our results only with caution.

Manubrial vibrations

Figure 5 shows manubrial displacement responses for gerbil H. We measured the umbo displacement at the start of the measurement series (black curve) and, to check for temporal effects, we measured it again 32 min later at the end of the series (gray curve). Comparison of the two umbo responses shows that the details were almost completely preserved, indicating that temporal effects were very small over the time period required to measure all of the points on the manubrium. As mentioned in the “Low frequencies” section under “Umbo and pars flaccida vibrations”, the state of the pars flaccida in this ear changed from flat (Fig. 4) to retracted (Fig. 5). As seen in this figure, all points along the manubrium moved in phase with each other (within 5°) up to at least 5 kHz, while the magnitude increased from the lateral process to the umbo. Similar differences along the manubrium were observed in all ears. This gradual increase is consistent with the classical view of rotation of the malleus around a fixed axis of rotation.

In order to estimate the position of the axis of rotation from the experimental data, we used an improved version of the 3-D gerbil middle ear model of Gea et al. (2009), reconstructed based on a micro-CT dataset. We oriented the model to correspond to the angle of view in our experiments and then used it to estimate the distances between the measurement locations on the manubrium. Using the ratio of the displacement magnitude of the umbo to that of the lateral process of the malleus (Fig. 5) averaged over the frequencies from 0.3 to 4 kHz and using distances taken from the model, the low-frequency axis of rotation was estimated to be approximately 1.7 mm superior to the lateral process of the malleus, measured along an extension of the line from the umbo to the lateral process (as projected onto the plane perpendicular to the direction of the laser beam). In the 3-D model, the anatomical axis of rotation (running from the tip of the anterior malleal process to the posterior incudal ligament) is estimated to lie approximately 1.9 mm superior to the lateral process of the malleus (measured along a line in the same direction as described previously). This is quite comparable to the value of 1.7 mm found from the experimental data. It should be noted that, for an accurate estimation of the location and orientation of the axis of rotation, 3-D measurements like those of Decraemer et al. (1994a, 2011) are required.

In our results, for frequencies higher than 5 kHz, the trend continues of increasing displacements from the lateral process to the umbo, but phase differences among the points along the manubrium start to become more evident, with the phase difference between the umbo and the short process increasing with frequency up to about 19° at 10 kHz. In Figure 4-B of de La Rochefoucauld and Olson (2010), a phase difference of about 7° at 5 kHz and a maximum phase difference of about 15° between the umbo and the lateral process in the range of 5 to 10 kHz can be seen, which is comparable to the findings here. They observed much greater phase differences at frequencies beyond those considered here.

These differences in phase indicate mode changes of the malleus and flexing of the tip of the manubrium at high frequencies, as can be seen in Figure 6 for gerbil H (as in Fig. 5) and gerbil K. In this figure, the displacements of the points on the manubrium are drawn for four frequencies and for seven equally spaced time instants within each cycle. The manubrium appears to be moving more or less as a rigid body with a fixed axis of rotation at the lowest frequency (400 Hz). In gerbil H at 1,600 Hz, the manubrium again appears to be almost rigid and the axis of rotation is again almost fixed at the same position as for 400 Hz. At this frequency in gerbil K, however, the

axis of rotation clearly moves throughout the cycle. Non-straight lines seen at 8,600 and 9,500 Hz can be attributed to flexing in the region of the umbo, changes in the rigid-body vibration mode of the malleus, or both. Our data are consistent with a recent study by Decraemer et al. (2011) in which complex motions of the gerbil malleus were observed.

Pars tensa vibrations

As described in the “Measurement and analysis procedures” section, vibrations of the pars tensa were studied by placing beads on its posterior and anterior parts at the level of the middle of the manubrium and in the region just posterior, anterior, and inferior to the umbo.

Low-frequency response. Figures 7 and 8 illustrate vibrations at the level of the middle of the manubrium in gerbils G and J. These figures show that points on the pars tensa and the manubrium move in phase up to about 2 kHz. The relationships among the magnitudes at the different points are more clearly shown in Figure 9, with the magnitudes of the pars tensa points in all ears, normalized by the respective displacements at the manubrium, at a low frequency (0.5 kHz). All curves have a minimum at the manubrium and, for approximately the same distances from the manubrium, beads on the posterior side show larger displacements than the ones on the anterior side. Note that, although the relative positions of the beads are approximately constant from ear to ear, we did not measure the actual distances between the measurement points, so the curves are presented based on bead numbers rather than positions.

High-frequency response. Beyond 2.1 kHz in Figure 7 and 1.9 kHz in Figure 8, different points of the pars tensa move out of phase with each other and the manubrium and show frequency-dependent magnitude differences, indicating that the simple vibration pattern has broken up. Table 1 shows the breakup frequencies for all ears, based on the frequency at which the phase curves for different points diverge by more than 15° (five times the short-term repeatability described in the “Repeatability and temporal effects” section).

Because of the length of the experiment and the difficulty of keeping the animal alive, measurements on both ears could only be done in one animal (gerbil G). Table 1 shows that both the resonance frequencies and the breakup frequencies of the two ears of this animal were very similar.

Figure 10 shows the pars tensa motions at the level of the middle of the manubrium in two ears at seven time instants throughout the cycle for four frequencies. In this figure, displacements were normalized by

the displacement magnitudes at the manubrium. The first row shows the low-frequency displacement at 0.5 kHz, with points moving in phase and displacement increasing when moving further away from the manubrium, similar to what was seen in Figure 9. The second row shows the displacements at the onset of breakup as defined earlier. At this frequency, the magnitude envelopes are still similar to the ones at low frequencies, but phase differences between points start to make the displacement pattern more complex. The last two rows show displacements at frequencies 1.3 and 1.5 times the breakup frequencies, respectively, that is, at 2.7 and 3.2 kHz for gerbil H and at 3.6 and 4.2 kHz for gerbil K. At these frequencies, the anterior and posterior parts vibrate in very different ways. In the posterior part, a displacement maximum appears at the second point from the manubrium. At the frequencies shown here, the phase differences seen from point to point indicate that there is no pure standing wave.

In addition to pars tensa points at the level of the middle of the manubrium, Figure 8 also shows the response of a point inferior to the umbo. The magnitude of motion of this point is comparable to the magnitudes of other points on the pars tensa, while its phase stays closer to that of the manubrium up to higher frequencies (within 16° up to about 4 kHz).

Figure 11 provides more data about the vibrations of the pars tensa in the region of the umbo for gerbil F. This figure confirms that, similar to responses of the pars tensa points at the level of the middle of the manubrium, responses in this region break up beyond a particular frequency. In this ear, a breakup frequency of 2.3 kHz is seen in the figure, which is the same as for points at the level of the middle of the manubrium

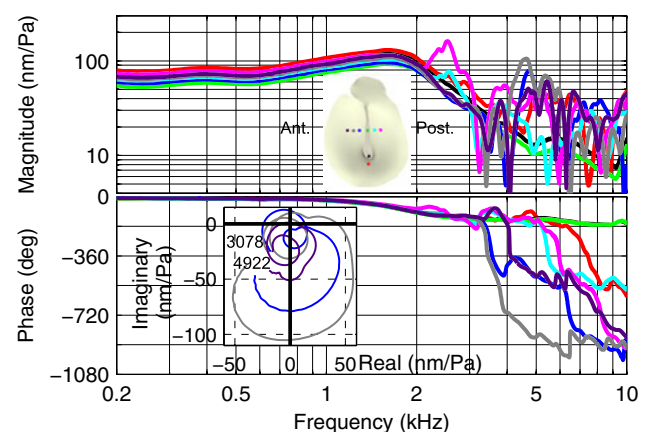


FIG. 8. Pars tensa displacement responses, normalized by sound pressure, at locations in a line perpendicular to the manubrium, at the umbo, and at a location inferior to the umbo in gerbil J. The inset shows the Nyquist plots for three anterior pars tensa points in the frequency range of 3,078 to 4,922 Hz, as discussed in the “Appendix.”

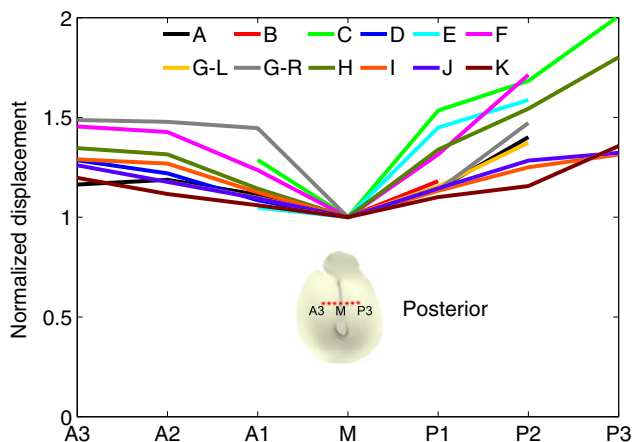


FIG. 9. Pars tensa motion at a low frequency (0.5 kHz) in all gerbil ears. The *horizontal axis* shows the bead number on the pars tensa, and the *vertical axis* shows the displacement magnitude normalized by that of the manubrium.

(not shown). The similarity of the phase in the inferior region to that at the umbo, seen in Figure 8 beyond the breakup frequency, is not seen here but was observed in some other ears.

DISCUSSION

Umbo and pars flaccida responses

Kohllöffel (1984) performed anatomical measurements of the pars flaccida and suggested that, among other possible roles, the pars flaccida may act as a shunt around the pars tensa at low frequencies in some species. Teoh et al. (1997) adapted Kohllöffel’s generic circuit model to the gerbil middle ear and determined model parameters based on their admittance measurements. They showed that the large pars

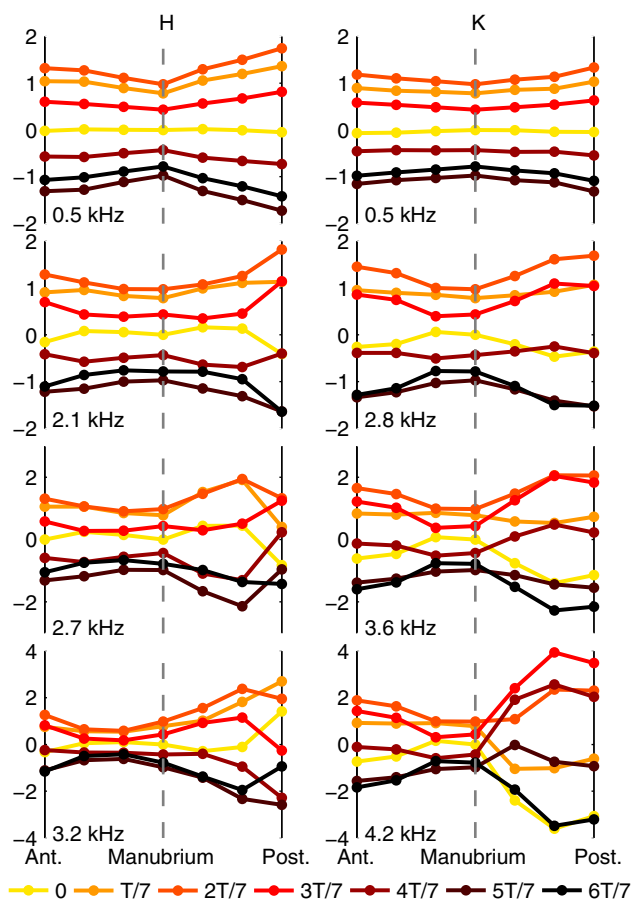


FIG. 10. Sinusoidal motion of the pars tensa points at the level of the middle of the manubrium at seven time instants (multiples of $T/7$) throughout the cycle in gerbils H and K at four frequencies (from top to bottom: low frequency, breakup frequency, 1.3 times the breakup frequency, and 1.5 times the breakup frequency).

flaccida in this species is responsible for reducing the hearing sensitivity around the pars flaccida resonance frequency, which is between 500 and 900 Hz in our observations, and at lower frequencies.

Our results confirm that a flat pars flaccida has larger displacements than the umbo, as was observed by Rosowski et al. (1997), and also show that it has larger displacements than the pars tensa in this low-frequency range. A flat pars flaccida is manifested by the presence of a distinct feature in the umbo response below 900 Hz: as the frequency approaches and passes the pars flaccida resonance frequency, the umbo magnitude response passes through a minimum and the phase passes through a maximum. Above its resonance frequency, the motion of the pars flaccida is more or less mass-dominated, and as it rolls off, its effect on the umbo response becomes negligible.

Near and above its resonance, the phase of the flat pars flaccida departs from that of the umbo and its

TABLE 1

Estimation of breakup frequencies in 12 gerbil ears

| Gerbil ear | Middle ear resonance frequency (kHz) | Breakup frequency (kHz) |
|------------|--------------------------------------|-------------------------|
| A | 2.0 | 2.3 |
| B | 1.7 | 2.5 |
| C | 1.6 | 1.9 |
| D | 1.8 | 2.8 |
| E | 1.6 | 1.8 |
| F | 1.9 | 2.3 |
| G—left | 1.9 | 2.1 |
| G—right | 2.0 | 2.2 |
| H | 1.9 | 2.1 |
| I | 2.0 | 2.8 |
| J | 1.7 | 1.9 |
| K | 1.8 | 2.8 |

magnitude remains higher up to about 4.5 kHz, except for an antiresonance in some ears. This antiresonance was not observed in all ears, presumably because it is very sensitive to the location of the bead near the center of the pars flaccida: a small difference between the bead locations from one ear to the other may cause the presence or absence of this feature. For frequencies higher than 4.5 kHz, the pars flaccida magnitude is either lower than or at the same level as that of the umbo.

When the pars flaccida is retracted inside the middle ear cavity, it becomes stiffer and cannot play its normal role of shunting low-frequency sound around the pars tensa. In this situation, at low frequencies, the umbo response looks like the response of a stiffness-dominated system. This is consistent with earlier observations of an artificially stiffened pars flaccida (Teoh et al. 1997; Rosowski and Lee 2002).

The phase of the retracted pars flaccida shows a divergence from that of the umbo at about 1.0 to 1.7 kHz accompanied by a minimum in the magnitude. Modeling studies may shed some light on the cause of this behavior. For frequencies beyond this feature, the response of a retracted pars flaccida is more or less like a mass-dominated system.

The umbo magnitude response shows a relatively broad resonance at about 2 kHz, indicative of heavy damping, followed by an overall decrease with irregularities. These irregularities are presumably the result of complex motions of the pars tensa (see the “Pars tensa vibrations” section) and of the ossicular chain (Decraemer et al. 2011).

Pars flaccida retraction

Some of the ears in this study had a retracted pars flaccida. (During measurements in two ears, we noticed that, over a time interval of about 1 min, the

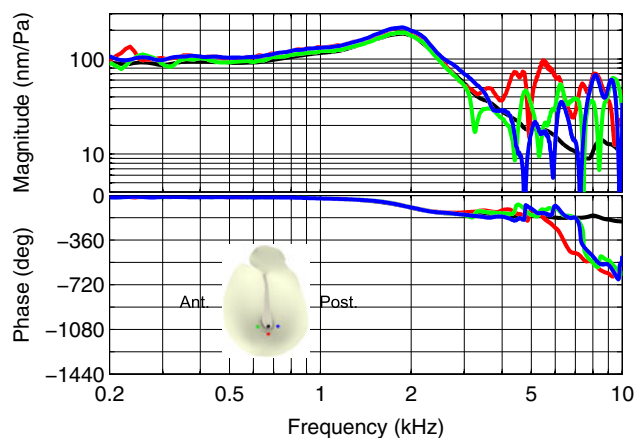


FIG. 11. Pars tensa displacement responses, normalized by sound pressure, at locations at the umbo and around the umbo in the left ear of gerbil F.

initially flat pars flaccida became retracted into the middle ear cavity.) So far, we have not been able to control the shape of the pars flaccida in vivo. Nambiar (2010) carried out a postmortem study on the gerbil TM in which rapid euthanasia by a carbon dioxide overdose was performed before the surgery was started. In that study, the pars flaccida was always flat and the pars flaccida effect was always evident in the umbo responses. Effects on the umbo response that are similar to those of pars flaccida retraction can be produced by applying static pressure to the middle ear cavity (Lee and Rosowski 2001) or by immobilizing the pars flaccida (Teoh et al. 1997; Rosowski and Lee 2002). In the impedance measurements of Ravicz et al. (1992), the distinctive umbo response feature caused by the pars flaccida was absent except in one ear. Teoh et al. (1997) attributed this absence to the effects of drying because Ravicz et al. (1992) did not moisten the pars flaccida. However, we also did not moisten the pars flaccida, and drying did not eliminate the pars flaccida effect. Therefore, it may be that the pars flaccida was retracted in most of the (1992) measurements but that the retraction was not noticed.

It has been seen in different species that, in the presence of liquid in the middle ear cavity, the pars flaccida is retracted into the cavity (e.g., Tos and Poulsen 1980, in humans; Stenfors et al. 1981, in rats; Larsson et al. 2005, in gerbils). Such retractions might have been caused by the development of negative pressures inside the cavity. Indeed, only a very small pressure is needed to retract the pars flaccida (Dirckx et al. 1998). Although negative pressure can initiate the retraction, it cannot be responsible for keeping the membrane retracted in our case because equalization of the middle ear pressure by creation of a ventilation hole in the cavity wall did not cause the flat shape to be recovered. Although we checked that our ventilation tubes were patent when inserted, as mentioned in the “Preparation” section, it is possible that they became blocked at some point in the two ears in which a previously flat pars flaccida became retracted after creation of the ventilation hole and insertion of the ventilation tube. However, removing the ventilation tube as soon as the retraction happened did not change the state of the pars flaccida. Indeed, we have observed that applying a positive static pressure to the ventilation tube moves the pars flaccida back to its natural flat state and causes the pars flaccida contribution to the frequency response to be recovered, but when the pressure is released, the pars flaccida is retracted again. The surface tension of a liquid film that forms on the cavity wall near the pars flaccida may pull it inward and keep it retracted. When the liquid film behind the pars flaccida is removed, the flat shape is recovered and maintained, but this removal requires a wide opening

of the cavity wall, which cannot be done until the very end of our data collection protocol. The removal also carries the risk of tearing the pars flaccida.

In the literature, different mechanisms have been suggested as being responsible for the emergence of liquid in the middle ear cavity. One of those mechanisms is the development of negative pressure inside the cavity. Flisberg et al. (1963) showed that, with a negative pressure of 20–30 mmHg, 15 min was enough for transudation to start in the human ear. Hiraide and Paparella (1972) and Hiraide and Eriksson (1978) reported that as little as 1 min at –5 mmHg in guinea pigs caused transudation. Hutchings (1987) applied negative pressure in the gerbil middle ear cavity for 30 to 90 min and observed that any pressure more negative than –11 mmHg caused transudation.

In our experiments, we used pentobarbital, which is known to disable the muscles of the eustachian tube (e.g., Doyle et al. 1995). Zheng et al. (1997) reported that pentobarbital caused negative middle ear pressure in gerbils, and they suggested that this might be due to the inactivity of the tube muscles. Occlusion of the eustachian tube is thus one of the candidates for causing the development of a negative pressure in the cavity and the subsequent accumulation of liquid. A good description of the underlying mechanism of the gas exchange process can be found in Sadé and Ar (1997).

Theoretically, nitrogen partial pressure dominates the gas exchange process in the long term and, even without a functional eustachian tube for the length of our experiments, it should not allow the development of large enough negative pressures to cause transudation. Doyle et al. (1999) measured the trans-mucosal gas exchange rate of nitrogen and calculated that opening of the eustachian tube once a day is enough to prevent middle ear effusion in monkeys. When Hiraide and Paparella (1972) closed the eustachian tube in guinea pigs and monkeys, they found that transudation did not occur in less than 24 h. Although these two studies suggest that negative pressures that are large enough to initiate transudation should not build up in short periods of time after eustachian tube occlusion, Eriksson et al. (2003) reported liquid in the middle ear within only 3 h of the occlusion of the eustachian tube in rats, which is consistent with the retraction of the pars flaccida during our experiments.

Another factor in our experiments is that the stream of oxygen that we kept in front of the animal's nose might have affected the gas exchange by causing hyperventilation, hyperoxia, and/or hypocapnia. It would be necessary to monitor the animal's respiration to confirm this.

Yet other mechanisms might be responsible for the emergence of liquid in the cavity. Alm et al. (1983)

demonstrated that mechanical scratching of the external ear canal in rats caused the emergence of liquid in the cavity and the ear canal and retraction of the pars flaccida within 30 min. They also showed that irritation of the ear canal with an airflow of 5 L/min at 15 °C had the same effect. Later, Hellström et al. (1985) studied the effect of airflow temperatures of 14, 24, and 34 °C and concluded that the phenomenon is temperature-dependent with the greatest effect at 14 °C and no effect at 34 °C, which is the normal temperature for the ear canal. Although their study emphasized the impact of temperature and they mentioned the similarity of the response to that of the mucosa of the bronchi and nasal cavity, they still attributed these effects to the irritation of the ear canal and not to the possibility of a temperature-related response of the middle ear mucosa caused by conductive heat transfer across the TM.

Our experiments involve both mechanical stimulation of the external ear and changes in temperature inside the middle ear cavity and ear canal. The temperature changes are caused by inserting the ventilation tube, which introduces air at room temperature into the cavity, and by removing the cartilaginous ear canal and attaching an aluminum coupler, the high thermal conductivity of which keeps the canal environment near room temperature.

In summary, although negative pressure may initiate pars flaccida retraction, we think that formation of a liquid film near the pars flaccida may be the cause of maintenance of the retraction and possibly also for its initiation. One or more of the mechanisms discussed previously may be responsible for the emergence of liquid in the middle ear cavity in our experiments. It remains unexplained, however, why retraction of the pars flaccida does not occur in some gerbils. Since the pars flaccida influences the responses of the manubrium and pars tensa, its status is very important for the interpretation of the measurements.

Manubrial response

The results presented here show that, for frequencies up to at least 5 kHz, the displacement magnitude increases from the lateral process to the umbo and all manubrial points move in phase with each other. The location of the axis of rotation that was calculated from experimental results at low frequencies was shown to be close to the location of the anatomical axis of rotation in a reconstructed 3-D model of the gerbil middle ear. Beyond 5 kHz, although the trend of increasing magnitudes is preserved, there is an increasing phase difference with frequency that may indicate a change of the vibration mode of the malleus and some flexing of the tip of the manubrium

consistent with observations in the cat (Decraemer et al. 1991, 1994b) and, more recently, in the gerbil (Decraemer et al. 2011). The flexing of the manubrium in the cat has been shown to be consistent with the geometry of the manubrium and with plausible material properties (Funnell et al. 1992), but a similar analysis has not been done for the gerbil. Changes in the vibration mode of the malleus are compatible in principle with the elastic suspension of the ossicles but have not yet been modeled quantitatively.

Pars tensa response

At low frequencies, we observed a fundamental mode with all pars tensa points moving in phase with the manubrium. The magnitude at the manubrium is lower than that on the pars tensa, and the posterior side tends to have larger displacements than the anterior side. The vibration pattern becomes more complex at higher frequencies, which is consistent with previous experimental results (e.g., Khanna and Tonndorf 1972) and modeling results (e.g., Funnell 1983). The breakup occurred between 1.8 and 2.8 kHz in the ears studied here, which is similar to what has been found in other species. These observations will be important for the development and validation of middle ear finite-element models for the gerbil, in conjunction with the 3-D ossicle measurements of Decraemer et al. (2011).

ACKNOWLEDGMENTS

The authors would like to thank Ms. Shruti Nambiar and Ms. Zinan He for their contributions to the development of the surgical and measurement techniques; Dr. Jim Gourdon for the advice on the anesthesia procedure; and Dr. Dan Citra for his help in dealing with the animals. This work was supported in part by the Canadian Institutes of Health Research, the Fonds de recherche en santé du Québec, the Natural Sciences and Engineering Research Council (Canada), the Montréal Children's Hospital Research Institute, the McGill University Health Centre Research Institute and the Research Fund of Flanders (Belgium).

APPENDIX

An inset in Figure 8 shows the Nyquist plots for three anterior beads in the frequency range of 3,078 to 4,922 Hz, as an example of their use for verification of the phase response as mentioned in the “[Measurement and analysis procedures](#)” section. The unwrapped phases shown for these three beads follow what the Nyquist plots display regarding the phase evolution, which can be described in terms of “phasors,” that is, vectors drawn from the origin to points on the Nyquist plot. When for increasing frequency the

phasor rotates clockwise, the phase angle decreases (becomes more negative), and vice versa. All three curves start in the same quadrant and end in that same quadrant, but the trajectories in between are quite different. At the beginning of the violet trajectory on the Nyquist plot, the phasor rotates clockwise through a small angle then counterclockwise, corresponding to a phase decrease up to about 3,300 Hz and then a phase increase up to about 3,650 Hz. After this frequency, it rotates clockwise, which corresponds to a decrease in phase up to a point where the phasor becomes extremely short and the trajectory becomes almost tangent to the real axis, at about 4,100 Hz. Approaching and passing this tangent zone, with the phasor still rotating clockwise and encircling the origin, causes a sharp drop in the phase plot, after which the phasor becomes longer and continues to rotate clockwise, corresponding to a smooth phase drop. (When the phasor becomes very short, a very small difference in the real or imaginary parts due to noise or frequency resolution can change whether it encircles the origin or not, which in turn causes a difference of 360° in the phase.) The phasors for the blue and gray trajectories start rotating clockwise and both of them make circles, but the gray trajectory encircles the origin while the blue trajectory does not. This corresponds to a continuous drop of the gray phase plot, but an increase at about 4 kHz in the blue phase plot.

REFERENCES

- ALM P, BLOOM G, HELLSTRÖM S, STENFORS L, WIDEMAR L (1983) Middle ear effusion caused by mechanical stimulation of the external auditory canal: an experimental study in the rat. *Acta Oto-Laryngologica* 96(1-2):91-98
- AZIZ PM, SORENSEN HV, VAN DER SPIEGEL J (2002) An overview of sigma-delta converters. *Signal Processing Magazine, IEEE* 13(1):61-84
- BIGELOW DC, SWANSON PB, SAUNDERS JC (1996) The effect of tympanic membrane perforation size on umbo velocity in the rat. *Laryngoscope* 106(1):71-76
- CHENG JT, AARNISALO AA, HARRINGTON E, HERNANDEZ-MONTES MS, FURLONG C, MERCHANT SN, ROSOWSKI JJ (2010) Motion of the surface of the human tympanic membrane measured with stroboscopic holography. *Hear Res* 263(1-2):66-77
- COHEN YE, DOAN DE, RUBIN DM, SAUNDERS JC (1993) Middle-ear development. V: development of umbo sensitivity in the gerbil. *Am J Otolaryngol* 14(3):191-198
- DECRAEMER WF, KHANNA SM, FUNNELL WR (1989) Interferometric measurement of the amplitude and phase of tympanic membrane vibrations in cat. *Hear Res* 38(1-2):1-17
- DECRAEMER WF, KHANNA SM, FUNNELL WR (1991) Malleus vibration mode changes with frequency. *Hear Res* 54(2):305-318
- DECRAEMER WF, KHANNA SM, FUNNELL WRJ (1994A) A method for determining three-dimensional vibration in the ear. *Hear Res* 77(1-2):19-37

- DECRAEMER WF, KHANNA SM, FUNNELL WRJ (1994b) Bending of the manubrium in cat under normal sound stimulation. *Proc Opt Imaging Tech Biomed* 2329:74–84
- DECRAEMER, W. F., KHANNA, S. M., & FUNNELL, W. R. J. (1999). Vibrations at a fine grid of points on the cat tympanic membrane measured with a heterodyne interferometer. EOS/SPIE International Symposia on Industrial Lasers and Inspection, Conference on Biomedical Laser and Metrology and Applications.
- DECRAEMER, W. F., DE LA ROCHEFOUCAULD, O., & OLSON, E. S. (2011). Measurement of the three-dimensional vibration motion of the ossicular chain in the living gerbil. In C. A. Shera & E. S. Olson (Eds.), *Proceedings of the 11th International Mechanics of Hearing Workshop* 1403:528–533
- DIRCKX JJJ, DECRAEMER WF, VON UNGE M, LARSSON C (1998) Volume displacement of the gerbil eardrum pars flaccida as a function of middle ear pressure. *Hear Res* 118(1–2):35–46
- DIRCKX JJJ, DECRAEMER WF (2001) Effect of middle ear components on eardrum quasi-static deformation. *Hear Res* 157(1–2):124–137
- DOYLE WJ, ALPER CM, SEROKY JT (1999) Trans-mucosal inert gas exchange constants for the monkey middle ear. *Auris Nasus Larynx* 26(1):5–12
- DOYLE WJ, SEROKY JT, ALPER CM (1995) Gas exchange across the middle ear mucosa in monkeys: estimation of exchange rate. *Arch Otolaryngol Head Neck Surg* 121(8):887–892
- ELLAHAM, N. N., AKACHE, F., FUNNELL, W. R., & DANIEL, S. J. (2007). Experimental study of the effects of drying on middle-ear vibrations in the gerbil. 30th Ann Conf Can Med Biol Eng Soc
- EMGÅRD P, HELLSTRÖM S (1997) An animal model for external otitis. *European Archives of Oto-rhino-laryngology* 254(3):115–119
- ERIKSSON P, MATSSON C, HELLSTROM S (2003) First forty-eight hours of developing otitis media: an experimental study. *Ann Otol Rhinol Laryngol* 112(6):558–566
- FLISBERG K, INGELSTEDT S, ÖRTEGREN U (1963) On middle ear pressure. *Acta Oto-Laryngologica* 56(S182):43–56
- FULGHUM RS, MARROW HG (1996) Experimental otitis media with *Moraxella (Branhamella) catarrhalis*. *Ann Otol Rhinol Laryngol* 105(3):234–241
- FUNNELL WRJ (1983) On the undamped natural frequencies and mode shapes of a finite-element model of the cat eardrum. *J Acoust Soc Am* 73:1657–1661
- FUNNELL WRJ, KHANNA SM, DECRAEMER WF (1992) On the degree of rigidity of the manubrium in a finite-element model of the cat eardrum. *J Acoust Soc Am* 91(4):2082–2090
- FUNNELL WRJ, LASZLO CA (1982) A critical review of experimental observations on ear-drum structure and function. *ORL* 44(4):181–205
- GEA SLR, DECRAEMER WF, FUNNELL WRJ, DIRCKX JJJ, MAIER H (2009) Tympanic membrane boundary deformations derived from static displacements observed with computerized tomography in human and gerbil. *J Assoc Res Otolaryngol* 11(1):1–17
- HELLSTRÖM S, GOLDIE P, SALÉN B, STENFORS L-E (1985) Mechanisms in middle ear effusion production caused by irritation of the external auditory canal. *Am J Otolaryngol* 6(3):220–222
- HIRAIDE F, ERIKSSON H (1978) The effects of the vacuum on vascular permeability of the middle ear. *Acta Oto-Laryngologica* 85(1–6):10–16
- HIRAIDE F, PAPAPELLA MM (1972) Vascular changes in middle ear effusions. *Archives of Otolaryngology—Head & Neck Surgery* 96(1):45–51
- HUTCHINGS, M. (1987) The gerbil as an animal model of otitis media with effusion. *J Physiol (London)*, 396:175
- ISHIHARA M (1989) Experimental study of vibration analysis in middle ear models by holographic interferometry. Effects of the cross-sectioned area of aditus on the vibration of tympanic membrane. *Nihon Jibiinkoka Gakkai Kaiho* 92(5):726–735
- KHANNA SM, TONNDORF J (1972) Tympanic membrane vibrations in cats studied by time-averaged holography. *J Acoust Soc Am* 51:1904
- KOHLÖFFEL LUE (1984) Notes on the comparative mechanics of hearing. III. On Shrapnell's membrane. *Hear Res* 13(1):83–88
- KONRÅDSSON KS, IVARSSON A, BANK G (1987) Computerized laser Doppler interferometric scanning of the vibrating tympanic membrane. *Scand Audiol* 16(3):159–166
- DE LA ROCHEFOUCAULD O, OLSON ES (2010) A sum of simple and complex motions on the eardrum and manubrium in gerbil. *Hear Res* 263(1–2):9–15
- LARSSON C, DIRCKX JJJ, BAGGER-SJÖBÄCK D, VON UNGE M (2005) Pars flaccida displacement pattern in otitis media with effusion in the gerbil. *Otol Neurotol* 26(3):337
- LEE C-Y, ROSOWSKI JJ (2001) Effects of middle-ear static pressure on pars tensa and pars flaccida of gerbil ears. *Hear Res* 153(1–2):146–163
- MAETA M (1991) Effects of the perforation of the tympanic membrane on its vibration—with special reference to an experimental study by holographic interferometry. *Nihon Jibiinkoka Gakkai Kaiho* 94(2):231–240
- NAMBIAR S (2010) An experimental study of middle-ear vibrations in gerbils. Master of Engineering thesis. McGill University, Montréal, Canada
- OKANO K (1990) Influence of liquid volume in the middle ear on tympanic membrane vibration (experimental study by holographic interferometry). *Nihon Jibiinkoka Gakkai Kaiho* 93(11):1847–1855
- QIN Z, WOOD M, ROSOWSKI JJ (2010) Measurement of conductive hearing loss in mice. *Hear Res* 263(1–2):93–103
- RAVICZ, M. E., & ROSOWSKI, J. J. (1997) Sound-power collection by the auditory periphery of the Mongolian gerbil *Meriones unguiculatus*. III. Effect of variations in middle-ear volume. *J Acoust Soc Am* 10:2135
- RAVICZ ME, ROSOWSKI JJ, VOIGT HF (1992) Sound-power collection by the auditory periphery of the Mongolian gerbil *Meriones unguiculatus*. I: middle-ear input impedance. *J Acoust Soc Am* 92(1):157–177
- RAVICZ, M. E., ROSOWSKI, J. J., & VOIGT, H. F. (1996) Sound-power collection by the auditory periphery of the Mongolian gerbil *Meriones unguiculatus*. II. External-ear radiation impedance and power collection. *J Acoust Soc Am* 99:3044
- ROSOWSKI JJ, CHENG JT, RAVICZ ME, HULLI N, HERNANDEZ-MONTES M, HARRINGTON E, FURLONG C (2009) Computer-assisted time-averaged holograms of the motion of the surface of the mammalian tympanic membrane with sound stimuli of 0.4–25 kHz. *Hear Res* 253(1–2):83–96
- ROSOWSKI JJ, LEE CY (2002) The effect of immobilizing the gerbil's pars flaccida on the middle-ear's response to static pressure. *Hear Res* 174(1–2):183–195
- ROSOWSKI JJ, RAVICZ ME, TEOH SW, FLANDERMEYER D (1999) Measurements of middle-ear function in the Mongolian gerbil, a specialized mammalian ear. *Audiol Neuro-otol* 4(3–4):129–136
- ROSOWSKI JJ, TEOH SW, FLANDERMEYER DT (1997) The effect of the pars flaccida of the tympanic membrane on the ear's sensitivity to sound. In: Lewis ER, Long GR, Lyon RF, Narins PM, Steele CR, Hect-Poiner E (eds) *Diversity in auditory mechanics*. World Scientific, New Jersey, pp 129–135
- SADÉ J, AR A (1997) Middle ear and auditory tube: middle ear clearance, gas exchange, and pressure regulation. *Otolaryngol Head Neck* 116(4):499–524
- STENFORS L, CARLSÖÖ B, WINBLAD B (1981) Structure and healing capacity of the rat tympanic membrane after eustachian tube occlusion. *Acta Oto-Laryngologica* 91(1–6):75–84

- SUEHIRO M (1990) Effects of an increase or decrease in the middle ear pressure on tympanic membrane vibrations (experimental study by holographic interferometry). *Nihon Jibiinkoka Gakkai Kaiho* 93(3):398–406
- TEOH SW, FLANDERMEYER DT, ROSOWSKI JJ (1997) Effects of pars flaccida on sound conduction in ears of Mongolian gerbil: acoustic and anatomical measurements. *Hear Res* 106(1–2):39–65
- TONNDORF J, KHANNA SM (1972) Tympanic-membrane vibrations in human cadaver ears studied by time-averaged holography. *J Acoust Soc Am* 52:1221
- TOS M, POULSEN G (1980) Attic retractions following secretory otitis. *Acta Oto-Laryngologica* 89(3–6):479–486
- VON UNGE M, DECRAEMER W, BAGGER-SJÖBÄCK D, VAN DEN BERGHE D (1997) Tympanic membrane changes in experimental purulent otitis media. *Hear Res* 106(1–2):123–136
- VON UNGE M, DECRAEMER WF, BAGGER-SJÖBÄCK D, DIRCKX JJ (1993) Displacement of the gerbil tympanic membrane under static pressure variations measured with a real-time differential moiré interferometer. *Hear Res* 70(2):229–242
- VOSS SE, ROSOWSKI JJ, MERCHANT SN, PEAKE WT (2000) Acoustic responses of the human middle ear. *Hear Res* 150(1–2):43–69
- WADA H, ANDO M, TAKEUCHI M, SUGAWARA H, KOIKE T, KOBAYASHI T, HOZAWA K ET AL (2002) Vibration measurement of the tympanic membrane of guinea pig temporal bones using time-averaged speckle pattern interferometry. *J Acoust Soc Am* 111:2189
- ZHENG Y, OHYAMA K, HOZAWA K, WADA H, TAKASAKA T (1997) Effect of anesthetic agents and middle ear pressure application on distortion product otoacoustic emissions in the gerbil. *Hear Res* 112(1–2):167–174